DFIG Based WT for Frequency Control along with AGC in Multi-Area Systems

Om Prakash Bharti[1], Aanchal Verma[2], R. K. Saket[3,*], and S. K. Nagar[3]

ARTICLE INFO

Article history:
Received: 1 April 2020
Revised: 18 June 2020
Accepted: 3 August 2020

Keywords:
Doubly Fed Induction Machine (DFIG)
Wind Energy Converter System (WECS)
Automatic Governor Control (AGC)
Control error area (ACE)
Integral Square Error (ISE)

ABSTRACT

This paper focuses on Automatic Governor Control (AGC) operational and design perspectives for frequency control in multi-area systems. The transfer function model of the two-area scheme using a minute-perturbation transfer function model is discussed in this paper. The wind turbine (WT) containing a doubly fed induction generator (DFIG) is considered in this study of frequency control. The optimal tuning of DFIG controllers is also focused on in this paper. The optimal tuning process is very complicated due to the involvement of additional tuning parameters. The complete simulation analysis of optimal tuning of DFIG controllers and frequency control of the two-area system using AGC has been demonstrated. Furthermore, the analyses have been demonstrated to evaluate the system impingement of 20% and 50% penetration for wind generation.

1. INTRODUCTION

Energy is the most significant factor that sustain to impact the profile of progress in the 21st Century. Amongst the renewable energy resources, wind energy production machinery has been developed significantly. The wind is reasonably scattered in the region of the earth. All through modern year's vestige fuel imaginations are inadequate and have a momentous unpleasant impact on the surroundings through arousing CO2 stage in the environment as well as leading to climate change. In the midst of renewable energy sources, wind is the most capable resource. The share of wind-established power creation in entire power invention, the unit has been rising constantly in the globe. However, renewable energy would be offer up to 10 percent of energy of the world contribute in 2020 and increase up to 50 percent near 2050 [1,4].

In this manuscript, the attempt is made to revisit and track the position, through various degrees of the wind penetration, of variable-speed-based WTs, in the DFIG carefully, and in frequency regulation plus power. The price and accessibility of energy much effects our class of life, the fitness of state economies and the strength of our situation. In present there has been a huge worldwide declaration to construct up hygienic plus another types of resources of energy, furthermore it is imagined that by 2020, 10 percent of globe energy will be given from sustainable assets. There is an assumption that this worth will develop to half by 2050 [2, 3]. Wind power production was the world's main rising source of electricity in the earlier decade. In the other side, the additional distribution of wind power into the lifts provided by power plant managers and controllers. Wind turbo typically does not lead to frequency control or AGC administrations, and so a massive wind turbine input will impact total system inertia and frequency response intensity in turbulence [5, 6, 7, 31, 32]. The goal of this paper is to present mixed-generation network mathematical models along with different assumptions of penetration to obtain the control approach for the control of both primary and secondary frequency. The technique to enhance the system's dynamic response is also provided alongside single and two area frequency control. Several researchers have focused on wind turbines of DFIG-based to demonstrate their ability to incorporate different reactive and active power controls. In [8, 9] the concept of release of the kinetic energy of the wind turbine of DFIG-based was implemented, where the frequency of the power mechanism is simplified to prevent system inertia delimitations. The paper indicates that the wind turbine control system should employ an external power set-point. Dependent on the rate of frequency variation coupled with network inertia, this additional power relation

[1]*Department of Electrical Engineering, Government Polytechnic Ghazipur, U.P., (233001), India*.
[2]*Department of Electronics Engineering, Indian Institute of Technology (Banaras Hindu University) Varanasi, U.P., (221005), India*.
[3]*Department of Electrical Engineering, Indian Institute of Technology (Banaras Hindu University) Varanasi, U.P., (221005), India.*
**Corresponding author:* R.K. Saket; Phone: +91-9451067022; E-mail: rksaket.eee@iitbhu.ac.in.

is expected. The surplus power provided by the turbine helps to regulate the primary frequency, thus preventing the depletion of inertia of the system. The investigational findings of the engineering and construction of wind turbines of DFIG-based are provided in [10, 33]. The related rotor-side approach allows for optimum speed monitoring towards a large operating speed range. A model is proposed in [11] to present the two most relevant conceptions of variable-speed wind turbines in complex simulations of the power grid. The effect evaluation of high wind energy penetration into the system [12] is presented in view of the main impacts of limited wind saturation. The paper analyses the transient frequency between fixed-speed turbines and wind farms. Only minimal inertial assistance and variable-speed machines can be offered [8, 12]. A control strategy is proposed in [13, 28] that enables wind turbines of DFIG-based to contribute effectively to the regulation of system frequency. There is a demonstration in [14] of the inertial response of wind turbines using induction engine generators. The kinetic energy extraction theory of DFIG machinery is described in [15, 23] by reducing the speed of the rotor. Furthermore, the DFIG's rotational speed decreases and the output power decreases when the support of frequency control is stopped.

This paper's organisation is as follows. Section-1 outlines the underlying theory associated with non-conventional sources along with the wind energy conversion system. Functional framework of the wind energy conversion system along with DFIG-based wind turbine as well as restrictions on DFIG involvement in frequency control The assumptions are presented in Section-2. As stated in Section-3, the mathematical simulation of the power generation speed control system along with wind turbine models is described. In Section-4, the DFIG-Based Wind Turbine Control Model is provided along with Optimum Tuning Controller Parameters and Automated Governor Control with simulation performance. Section-5 outlines the DFIG-based WT Frequency Control model for Two Area Systems, along with simulation data. Finally, in the Section-6, observations and short discussions on field work are explained.

2. EFFICIENT CONFIGURATION OF WECS

For the WECS gearbox is the significant portion which is located between the principal shaft and the generator. It increases the spinning speed between 1000 and 1500 of the rotor blades (rpm). For the consumption of reactive type power, the capacitor banks are used. The WT coupling with variable power supply to the mains with invariable frequency is provided by power electronic converters [18]. The horizontal axis wind turbine as well as available wind turbines in the market given in fig.1 and in table 1 respectively.

Fig. 1: Horizontal axis wind turbine.

Table 1: Existing wind turbines in available the marketplace

Application	*Hub-Height in meter*	*Diameter in meter*	*Power Rating in MW*
Commercial	50-90	47-90	0.66-2.00
Medium	35-50	13-30	30KW-0.66
Residential	18-37	1-13	Below 30

The WECS might be assorted as by constant and variable-speed wind turbines [19]; (I) WECS with WTs at Fixed Speed (II) WECS with WTs at Variable Speed (III) WECS with Full Converter (IV) WECS with DFIG Based WT.

DFIG Based WT for WECS

The DFIG based WT along with the full load convertor connected is shown in Fig.2 for the most regularly applied variable speed generator drive conceptions with operating principle [20]. In comparison, the other drive types are still included in the souk, even though they are not actually used for WECs. Asynchronous generators are likely to be used for illustration in order to achieve variable speed in a generator push.

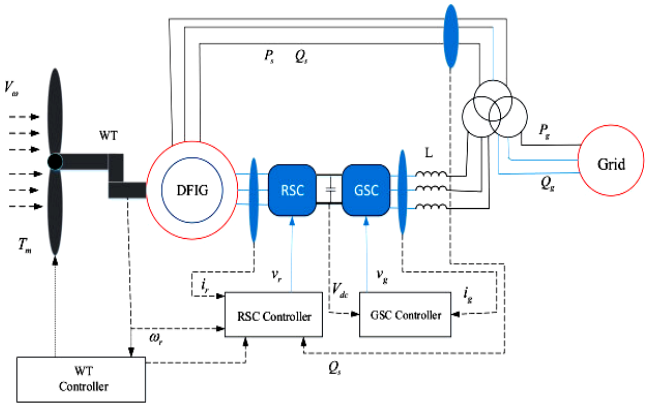

Fig. 2: DFIG based wind turbine for WECS.

Hypothesis and restriction for DFIG based WT in frequency regulation

The mechanical capacity of DFIG-based WT was believed to be invariable (wind velocity) in this work, so that volatility of wind power output was not conceived. It is also believed that, amid interruptions, conventional generation will provide the increased demand and increase the output required by mixed generation in the energy system. The system of Maximum Power Monitoring (MPT) pursues the optimum mechanical velocity and provides for transient divergence from the optimum velocity.

3. MODELING OF THE POWER GENERATING SYSTEM

The Speed Governing System

Fig. 3 demonstrates an extremely graphical mode of a speed regulating framework. The key elements of the speed control system are set out in [22, 24] as follows.

Speed Governor: This forms the heart of the speed governing system. It's a moving part coupled to the main shaft, it measures continuously the frequency (or speed). It is provided with two fly balls as shown in Fig.3. Any change in the speed will result in motion of these fly balls, on account of centrifugal force, towards each other decreased speed or away from each other increased speed. Ultimately the coordinate x_B will be affected which will result in change in main valve position through linkage mechanism.

Linkage Mechanism: It consists of two ABC and CDE rigid bonds, hinged at points B and D. The feedback is given by the L4 connection. Stiffly coupled are the linkage arms L1 and L2, and so are the arms L3 and L4. The four linkage points are all open.

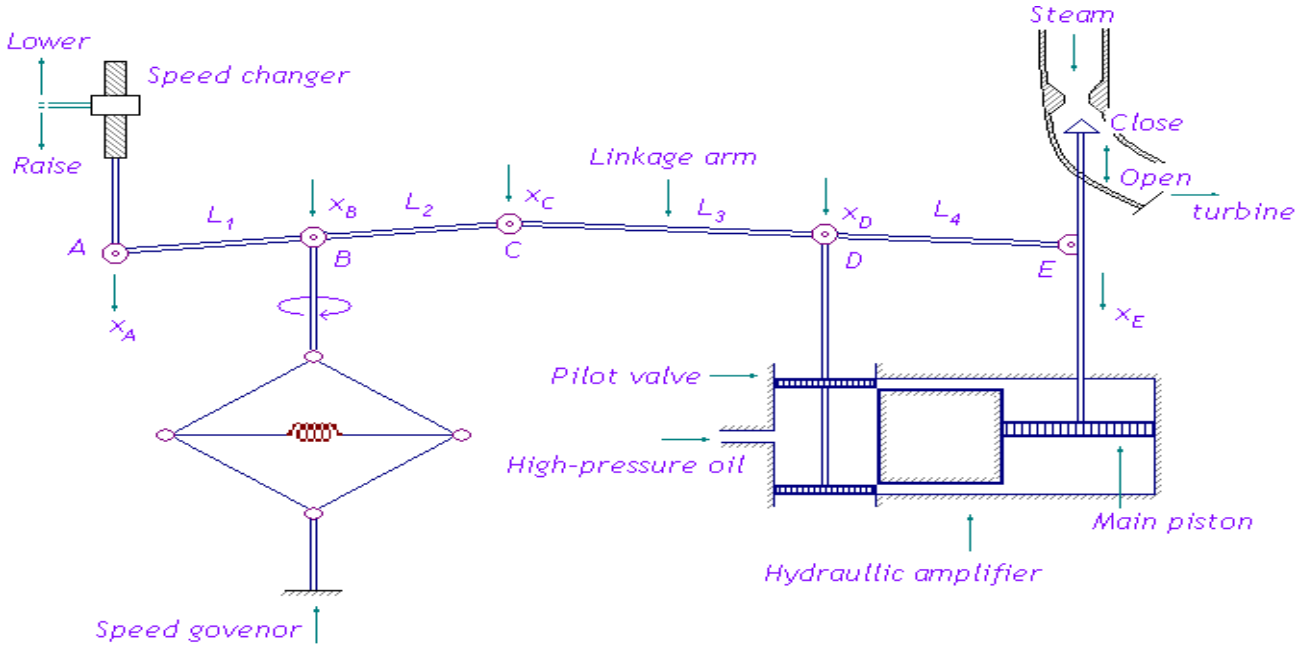

320

Fig. 3: Functional diagram of governor control loop.

Hydraulic Amplifier: Through several phases of hydraulic amplifiers, these forces are received. It is made up of two cylinders, one pilot valve and one main valve. This transforms the low power signal (movement of the pilot valve) to a high-power signal (main valve movement). The place x_D of the pilot valve is the input to this amplifier. The position x_E of the main piston is the output. The force amplification is very high because of the high-pressure hydraulic fluid exerting only a small differential force on the pilot valve. Via the connection device, the piston of the pilot valve can be influenced in three ways: directly, by shifting the connection point A by raising or lowering the velocity changer commands; indirectly, by feedback, by adjusting the direction of the main piston; and indirectly, by feedback, by changing the location of the connection point B due to velocity changes.

Speed Changer: The speed changer gives the continuous status of the speed control system. In order to change the reference setting (steady state operating point) 'Raise and lower' commands are given to speed changer and this command is translated into opening and closing steam valve (gate) through linkage mechanism and hydraulic amplifier.

Modelling of Speed Governing System

Consequently, assume the following sequence of events [22, 24] for the statistical modeling of the velocity regulating system.

(i) Initially, the device is in a constant steady state, characterized by a constant nominal frequency speed, x_E^o constant prime mover valve configuration, and P_G^o constant generator output capacity.

(ii) We order a power raise by speed changer, ΔP_c. As a consequence of this instruction, a small distance Δx_A relative to ΔP_c is pushed downward by the point A of linkage.

(iii) Small location shifts Δx_C and Δx_D of points C and D are triggered by the rotation of linkage point A. The steam valve will shift the small distance Δx_E as oil flows through the hydraulic engine, hence increases torque and, subsequently, a ΔP_G increase in power.

(iv) An additional power in the system, is caused by additional power demand. If the device is large in size, the surplus power will not greatly affect either the velocity or frequency, which will allow the velocity and point B to travel down a small distance of Δx_B relative to Δf. The pace governor, who is hasty, then neglects any delay in it. As a consequence, we set Δx_B proportional to Δf. All the gradual motions from, Δx_A, ..., Δx_E, are believed to be positive in the specified directions.

Since all the movements of the connection are minimal, the linear relationship is as given in (1)

$$\Delta x_C = k_1 \times \Delta f - k_2 \times \Delta Pc \ ,$$
$$\Delta x_D = k_3 \times \Delta x_C + k_4 \times \Delta x_E \quad (1)$$

The k_1 and k_2 values depend on the lengths of the arms 1 and 2 and on the speed changer and speed controller proportional constants. The k_3 and k_4 values depend on the lengths of the arms 3 and 4 of the linkage. If we assume that the flow of oil through the hydraulic motor is proportional to the pilot valve position Δx_D, the following relationship is obtained for the main piston position:

$$\Delta x_E = k_5 \int \Delta (-\Delta x_D)\, dt \quad (2)$$

The positive invariable k_5 depends on lips as well as cylinder geometries along with fluid force.

By taking the Laplace transform of Eqns. (1) and (2), and eliminating the variables Δx_C and Δx_D, the following equation is obtained.

$$\Delta x_E(s) = \frac{k_2 k_3 \Delta P_c(s) - k_1 k_3 \Delta F(s)}{k_4 + s/k_5} \quad (3)$$

Eqn. (3) can be rewritten as given in Eqn. (4)

$$\Delta X_E(s) = K_G/(1 + sT_G) \times [\Delta P_c(s) - \Delta F(s)/R] = G_G(s)[\Delta P_c(s) - \Delta F(s)/R] \quad (4)$$

where, $R = k_2/k_1$ = speed 'regulation 'due to governor stroke, $K_G = K_2 k_3 / k_4$ = static gain of speed-governing mechanism, $T_G = 1 / k_4 k_5$ = time constant, $G_G(s) = K_G / (1 + sT_G)$ = transfer function of speed-governing mechanism, T_G: is a measure o the reaction speed of the mechanism. Normal values are less than 100 ms.

Turbine Model

The turbine model descriptions in details are presented in [22,24] as follows. The objective of this paper is not primarily interested in turbine valve position per sec, but rather the resulting generator power increase ΔP_G. The adjustment in the position of the valve, Δx_E, induces a gradual increase in turbine capacity, ΔP_T, which would result in an increased generator power, ΔP_G, by electromechanical interactions within the generator. This overall process is relatively complicated, particularly if, due to significant network disruptions, the generator voltage undergoes wild swings simultaneously.

If, as in the present case, the voltage level can be assumed to be constant and the torque fluctuations are minimal, then an incremental study of the speed controller would provide a very simple dynamic relation between Δx_E and ΔP_G. Such a study shows major variations, not just between steam turbines and hydro turbines, but also between different steam turbine types (reheat and non-reheat). A non-reheat turbine generator can be described in Eqn as given in the crudest model Eqn. 5 for one K_T element of gain and T_T time constant.

$$G_T(s) = \frac{\Delta P_G(s)}{\Delta X_E(s)} = \frac{K_T}{1 + sT_T} \quad (5)$$

Usually, the time constant T_T lies in the range 0.2 to 2 s. In standard block-diagram symbols, Eqns. (2) and (5) can be represented as shown in Fig.4, thus the linear n 321 including the speed governor mechanism, reflects reheat-turbine controller.

The turbine power, ΔP_T, will be used for four different purposes:

(i) To deliver the requested 'new' load ΔP_L.

(ii) The kinetic energy, W_{kin}, of the unit is enhanced to accelerate the turbine-generator.

(iii) In order to maximize the capacity of outgoing lines, i.e., ΔP_l.

(iv) To accommodate the increase in the 'old' load.

The complete block diagram representation of control area is shown in Fig.5.

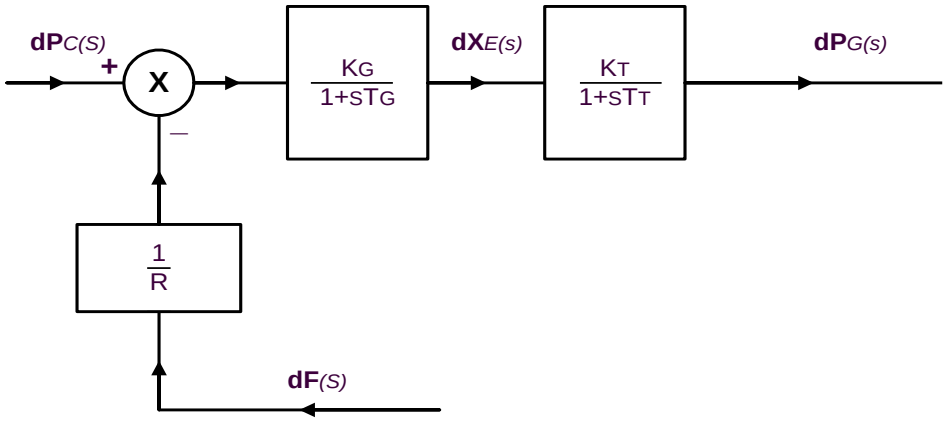

Fig. 4: Transfer function representation mechanism for generator power control.

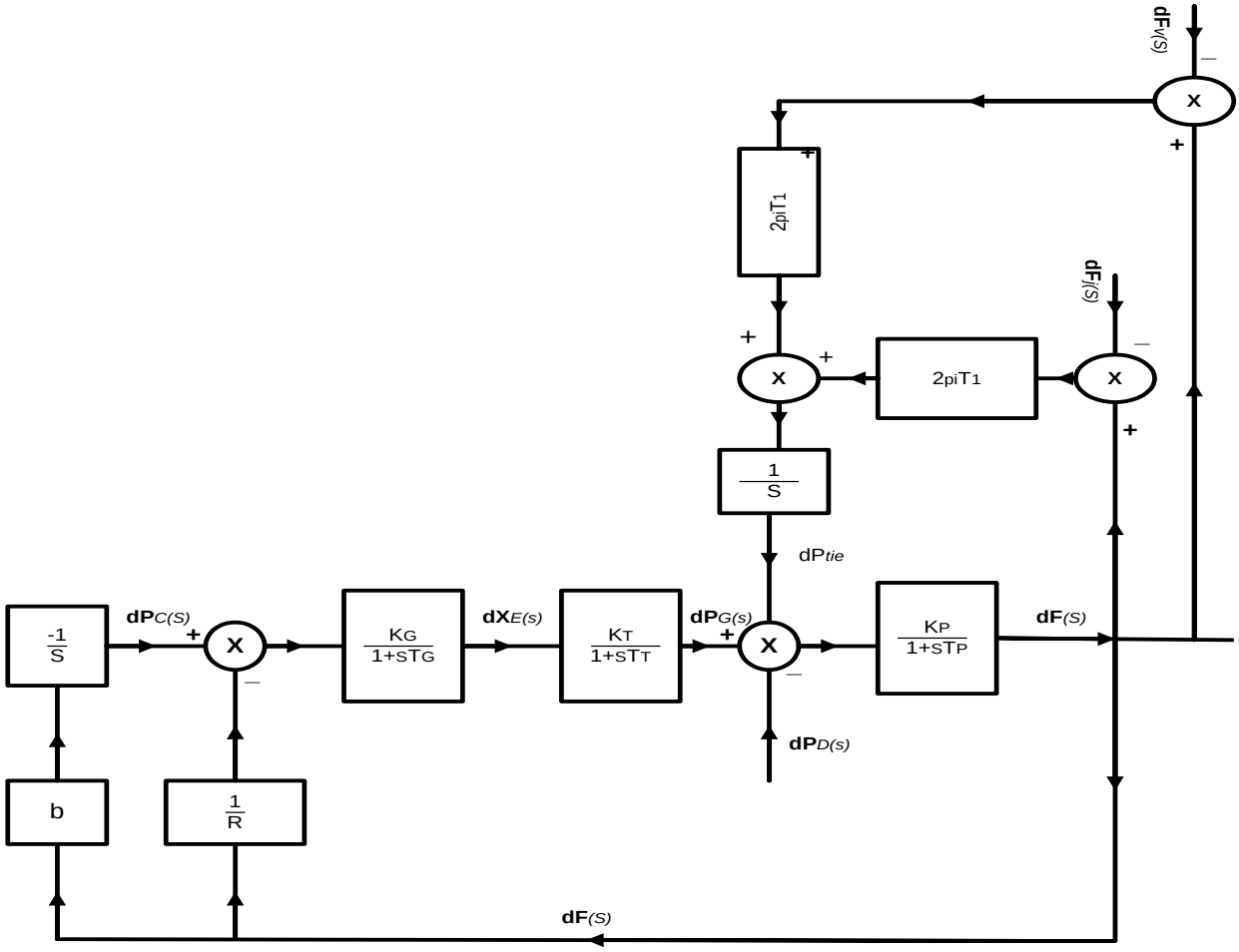

Fig. 5: Complete block diagram representation of control area.

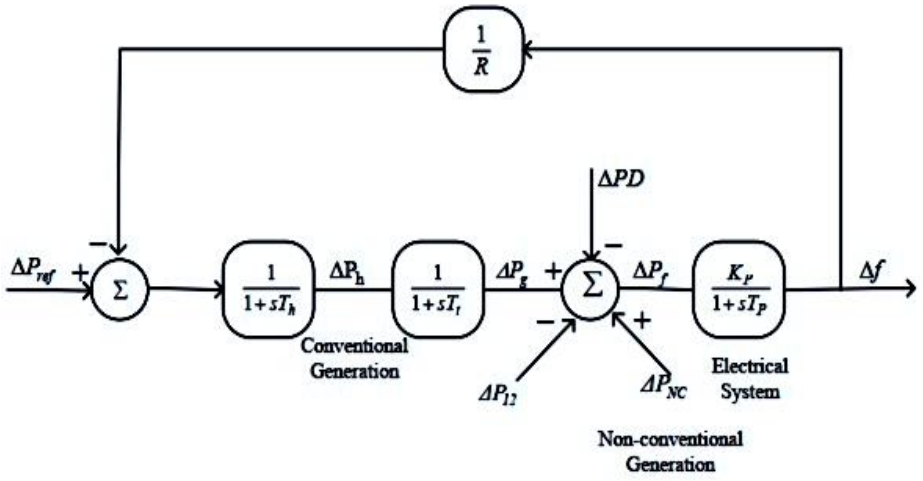

Fig. 6: Power system dynamic model indication with mixed generation.

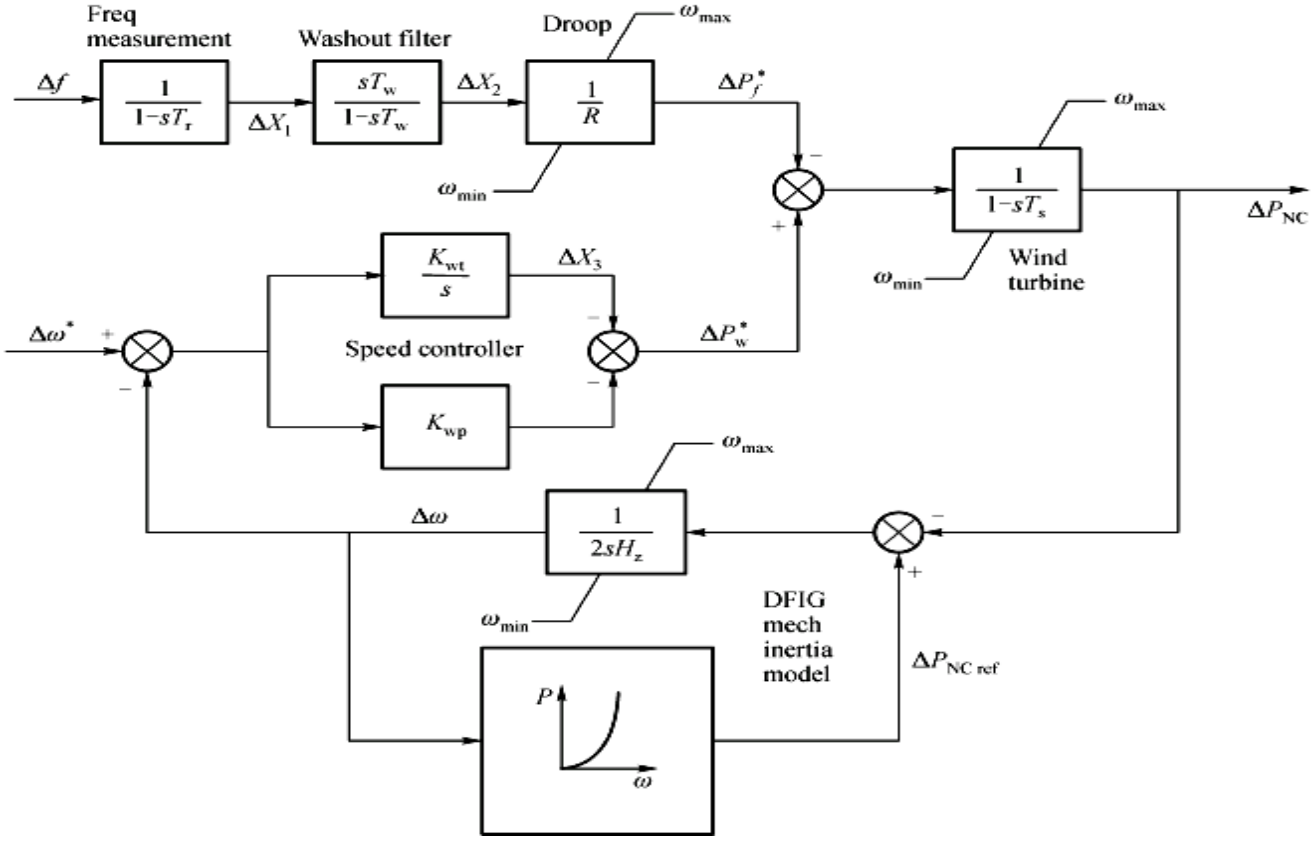

Fig. 7: DFIG-based wind turbine control established on frequency change.

4. DFIG-BASED WIND TURBINE CONTROL MODEL

The total transfer-function block diagram of a power system containing a traditional frequency control generator and a non-conventional wind turbine of DFIG-based generator contributing to the regulation of frequency is shown in Fig. 6. Increased active power demand ∇P_D subtracted from traditional generation increased values ∇Pg and wind generation ∇P_N is equal to the power transmitted from the neighboring area, ∇P_{12} as shown in Fig. 6 [12].

$$\nabla P_g + \nabla P_{NC} - \nabla P_{12} - \nabla P_D = \nabla P_f \tag{6}$$

From Fig. 6,

$$T_p = \frac{2H}{f_D} \tag{7}$$

$$K_P = \frac{1}{D} \tag{8}$$

$$\frac{2H}{f}\frac{d\Delta f}{dt} = \Delta P_f - D\Delta f = \Delta P_g + \Delta P_{NC} - \Delta P_{12} - \Delta P_D - D\Delta f \tag{9}$$

$$(\frac{2H}{f} + K_{df} = 2H^*)\frac{d\Delta f}{dt} = \Delta P_g - \Delta P_{12} - \Delta P_D - (K_{pf} + D = D^*)\Delta f \tag{10}$$

The dynamic model assumed for the frequency control analysis by means of DFIG-based WT [12, 16, 25, 30, 34] is seen in Fig.7. This model is basically selected from the DFIG model of simulation of inertia provided in Fig.6.

The differentiation between the models seen in Fig.6 and Fig.7 is the extra reference power that is built based on the adjusted frequency by a washout filter coupled with the time constant T_ω. This depends on a traditional concert in a transient key control.

$$\Delta P_f^* = \frac{1}{R}\Delta X_2 \tag{11}$$

Here R is the drop constant as conventionally used and is the calculated frequency shift where the wind turbine is linked to the network, whereas in [25] the dynamic model for AGC explored with DFIG-based WTS was clarified.

Optimal tuning scheme for DFIG-based WT controller parameters

In order that the frequency control response from distortions can improve, the aim of this section is to establish the optimum speed control parameter configurations for the DFIG-based WT. For finding the ideal values of K_{wp} along with K_{wi}, the Integral Squared Error (ISE) [17, 27] scheme is used. To observe the effect of wind energy expansion on the system's overall energy source combining, a Penetration Index (α_ω) is calculated as follows.

$$\alpha_\omega = \frac{Total Wind Generation}{Total Generation, From All, Sources} * 100 \tag{323}$$

Here two cases of DFIG penetration are considered: α_ω = 20%, α_ω = 50%.

In this work, the main values of the state variable are a progressive change of their nominal values otherwise it will be negative because the mechanism is constant. At $t \to \infty$, the system reaches steady-state, the $X(t)$ introduces the deviations from its steady-state value of the state variable at any moment. There is therefore a quadratic output index which indicates the squared deviations for the state variables for this complex display of the system for some control parameters;

$$J = \int_0^\infty (X_1^2(t) + X_2^2(t) + ...X_n^2(t))dt \tag{12}$$

The frequency deviation errors square, as shown below, will be used as the output index to set the controller parameters.

$$J = \int_0^\infty (\Delta f^2(t))dt \tag{13}$$

The performance index J is calculated for statistical reasons with very limited numbers of discrete values over a great deal of time in advance of the continuous state as seen below.

$$J = \sum_{k=1}^{K} [\Delta f^2(t_0 + k\Delta t)] \tag{14}$$

By penetrating the minimum value of J at first K_{wi} the optimum value of controllers K_{wp} and K_{wi} is calculated by setting the minimum value and adjusting K_{wp} over a wide range. J declines as K_{wp} increases, hitting minimum J i.e. it can be observed. In addition, J_{min} is again increasing. K_{wp} and K_{wi} values, which have the minimum of J i.e. J_{min}, are ideal parameters for the controller.

Table 2 displays the criteria for the optimum DFIG controller in area 1 for 20 percent and 50% WT penetration of the device with a 0.02-unit load disruption.

Table 2: Controller gain settings (area-1)

Wind Penetration	K_{wi1}	K_{wp1}	$J_{1\min}$
20%	0.12	1.24	0.1210
50%	0.12	1.99	0.1236

Optimal Tuning Controller Parameters of WT along with ACE

The optimum setting parameters and ACE in the two-area power system of the DFIG based WT are described [17] for the proportional integral controller. The ISE approach is used in any field to optimize K_{wp} and K_{wi} settings for the DFIG. Whereas the squared index of the deviations in status is designed as follows the quadratic output index:

$$J = \int_0^\infty [X_1^2(t) + X_2^2(t) + X_3^2(t) + ... + X_n^2(t)]dt \tag{15}$$

The square of the ACE is built in this paper as the output index in favor of tuning the controller parameters in each region is as follows.

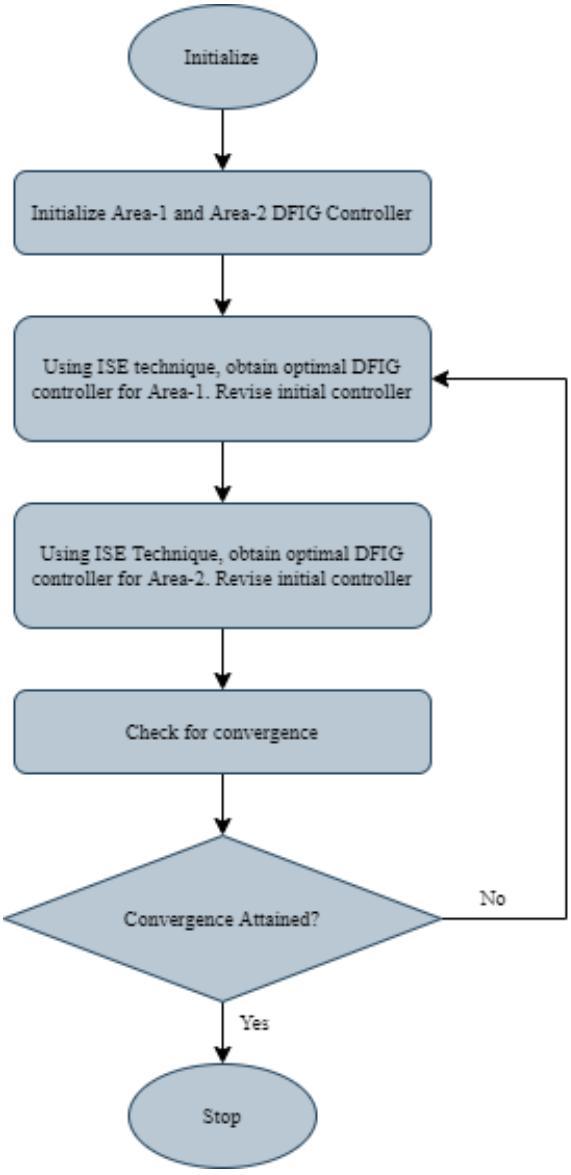

Fig. 8: Flow chart for optimal tuning DFIG controller parameter to both areas.

$$J_1 = \int_0^{\infty} (ACE_1)^2 dt \tag{16}$$

$$J_2 = \int_0^{\infty} (ACE_2)^2 dt \tag{17}$$

The performance index J is measured to help mathematical applications by using very small discrete values over a significant amount of time before reaching steady state as shown below.

$$J_1 = \sum_{k=1}^{K} [\Delta ACE_1^2(t_0 + k\Delta t)] \tag{18}$$

$$J_2 = \sum_{k=1}^{K} [\Delta ACE_2^2(t_0 + k\Delta t)] \tag{19}$$

Whereas in the two regions, the optimal gains are found by applying a iterative method that tries to lower the ACE's integral square error in each field. The step-by-step flow chart shows the perfect tuning process is shown in Fig. 8; K_{wp1} , K_{wi1} as well as K_{wp2} , K_{wi2} are decided [26]. According to the flow, the DFIG controller parameters for both areas were chosen at random first, and then the optimum gains for both areas were identified successively using the ISE procedure. For surety of the program achieves the optimal gains in support of the two controllers, a search for the integration of the optimal parameters is carried out. For optimum tuning, the flow map as seen in Fig. 8.

DFIG-based WT with Automatic Governor Control along with Simulation and results:

Fig. 8 shows the Simulink model using MATLAB to test the DFIG wind turbine frequency control or the AGC results.

Dissimilar plots for theses simulations are demonstrated in Fig.10 and Fig.11. The Fig.11 depicts the frequency responses by means of AGC for 20% as well as 50% wind input with and without DFIG.

Table 3: Optimal controller settings parameters of DFIG for area-2

Penetration value	K_{wi2}	K_{wp2}	$J_{2\min}$
20%	0.1	1.0	0.0499
50%	0.1	1.0	0.0765

The frequency results are very similar with and without the DFIG and are improved with the reduction of the frequency expedition when DFIG contribution is conceived. The adjustment period is also increased for cases of 20% and 50% wind penetration by using the parameters of the DFIG tuning speed controller. The settling time with the higher wind penetration can be expected to be longer.

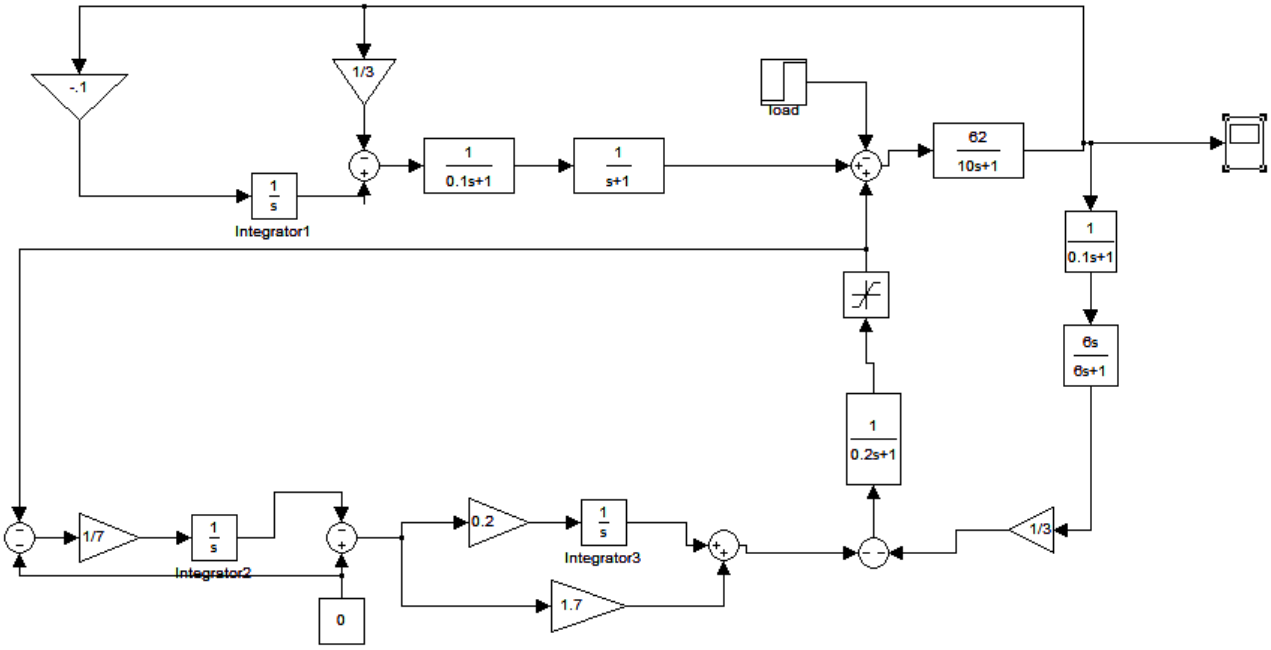

Fig. 9: DFIG based WT along with AGC simulation model.

5. FREQUENCY CONTROL IN 2- AREA SYSTEMS THROUGH DFIG-WT

For an integrated power grid, multiple-area frequency control effects are more important and convoluted than those combined with remote networks[12-16, 25, 29]. In remote networks, it is believed that the frequency throughout the network is invariant, resulting in one-area power. This is obviously not the case in immense interrelated networks where it is possible to distinguish many control areas. These control areas are conventionally related, along with their secondary frequency controls, to vertically integrated utilities for well-defined geographical areas.

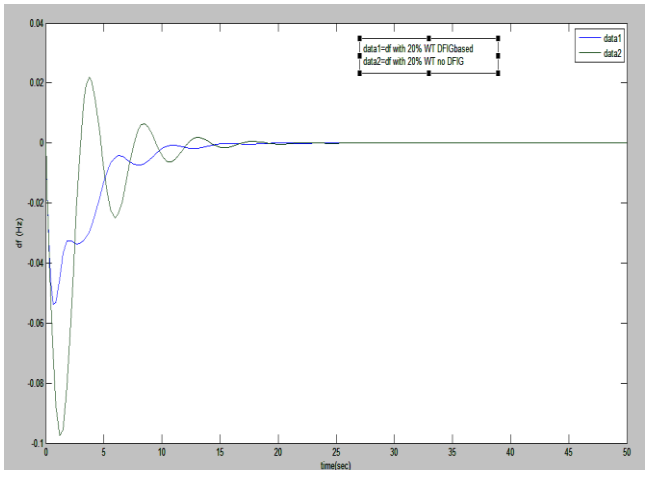

Fig. 10: AGC through 2% load increment with and without DFIG for 20% wind penetration.

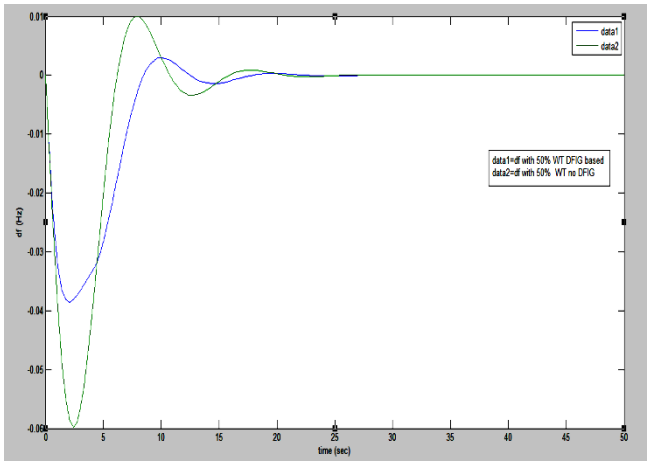

326 **: AGC through 2% load increment with and without DFIG for 50% wind penetration.**

Using the small-perturbation transfer-function model Fig.12, the complex efficiency of a two-area interrelated device may be investigated. After a disruption, this paradigm embraces both the main and secondary frequency modulation controls. In addition to system parameters as well as operating conditions, the system output is mainly affected by the integral control gains (K_{AGC1} and K_{AGC2}) along with the frequency bias factor (B_1 and B_2). Each region aims to bear its own load under standard working conditions. Single-area system frequency modulation is thus defined by the same frequency; Δf_1 and Δf_1 are therefore faced with gradual frequency shifts. Whereas, tie-line power flow is obtained in regular operation as:

$$P_{12}^0 = \frac{(|V_1^0||V_2^0|)}{X}\sin(\delta_1^0 - \delta_2^0) \quad (20)$$

where δ_1^0 and δ_2^0 are the angles of the tie ending voltages V_1^0 as well as V_2^0 correspondingly, furthermore P_{12}^0 is the tie line power. For a small value of δ_1 as well as δ_2 the increased tie line power is:

$$\Delta P_{12} \approx T_{12}[(\Delta\delta_1) - (\Delta\delta_2)] \quad (21)$$

$$T_{12} \overset{\Delta}{=} \frac{(|V_1^0||V_2^0|)}{X}\cos((\delta_1^0 - \delta_2^0)) \quad (22)$$

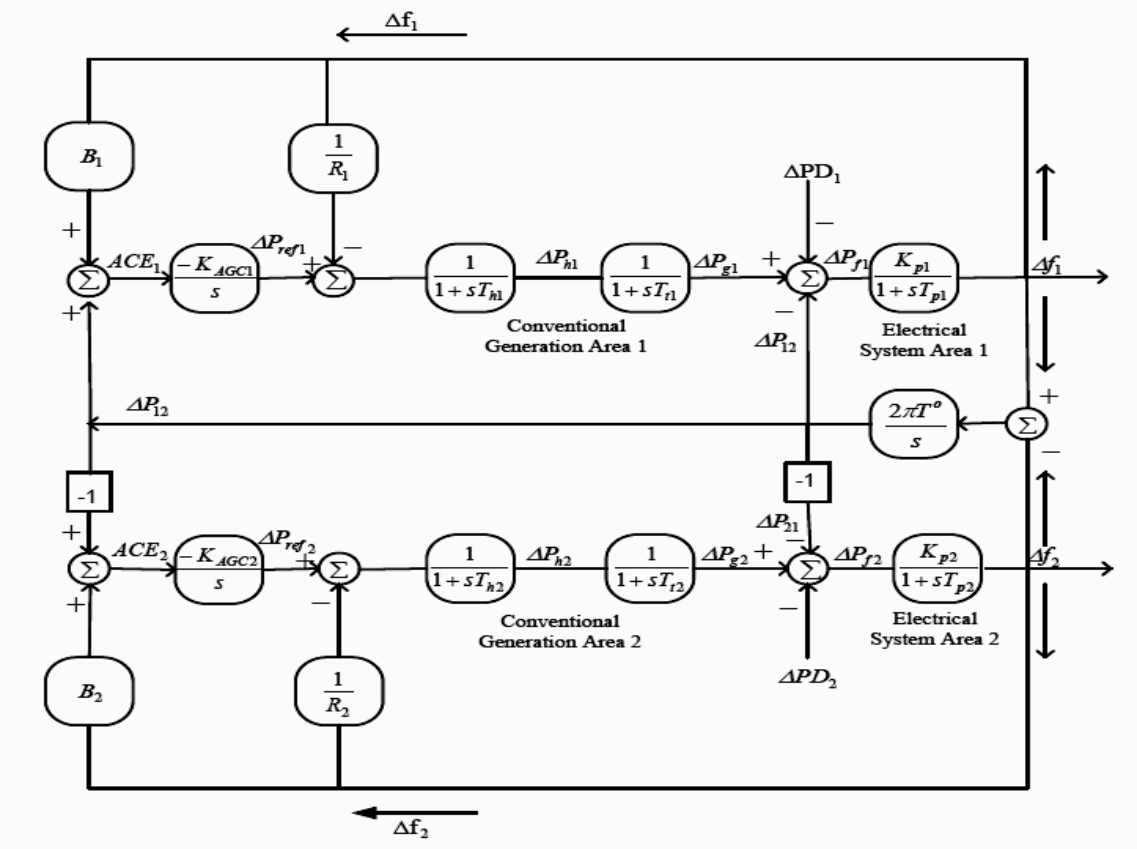

Fig. 12: Two Area Systems frequency control linear model.

[22, 24] have explained the synchronizing torque coefficient, same as the electrical stiffness principle in synchronizers.

The ACE for each area, on the other hand, for two area control systems, consists of a linear frequency combination along with a tie-line error as follows:

$$ACE_1 = \Delta P_{12} + B_1\Delta f_1 \quad (23)$$

$$ACE_2 = \Delta P_{21} + B_2\Delta f_2 \quad (24)$$

The dynamic model of frequency regulation for DFIG-Based WT_S has been described in [26].

Modelling of 2-area controller with DFIG-WT for frequency response

For the frequency response analysis, the MATLAB Simulink model of 2-area controller with DFIG-WT is shown in Fig. 13.

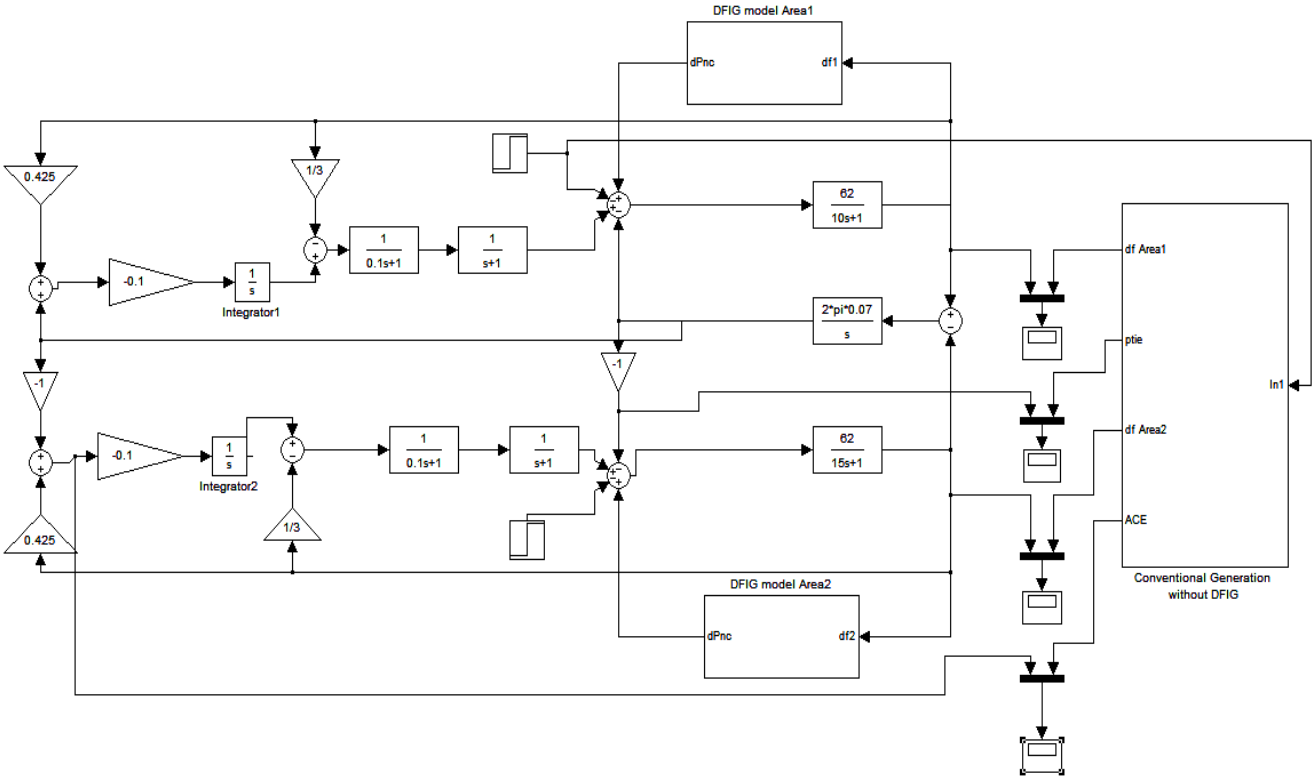

Fig.13: Simulink model of two-area controller with DFIG-based WT for frequency response studies

Frequency regulation Simulation results for two-area controller with DFIG-based WT

The simulations are carried out in order to determine its effect on the secondary frequency regulation, taking into account the optimum tuning DFIG controllers, the Simulink model as shown in Fig. 13 with the load disturbance of 0.02 per unit step. Fig. 14 to Fig. 21 show different plots for these simulations. For four instances of 20 percent as well as 50 percent of wind input with and without DFIG-WT, and the tie-line exponential power transition is presented in Fig. 16 and Fig. 20. The ACE plots for phase load disturbance are shown in Fig. 17 and Fig. 21.

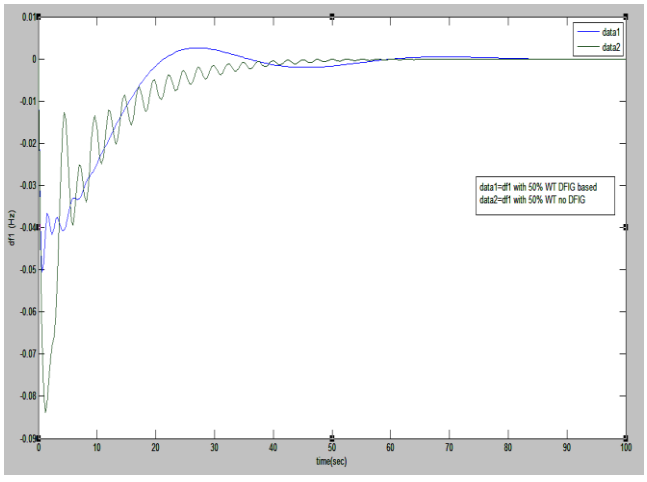

Fig. 14: Frequency regulation with and without DFIG for 50% wind penetration to area 1.

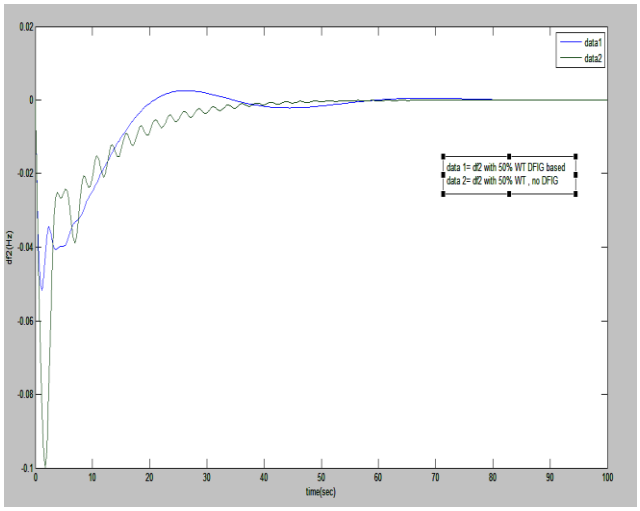

Fig. 15. Frequency regulations with and without DFIG for 50% wind penetration to area 2.

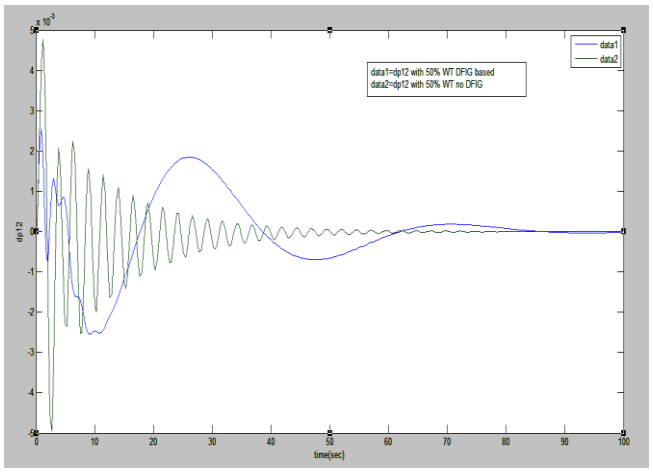

Fig. 16: Frequency regulation tie line incremental power for 50% wind penetration to area 1.

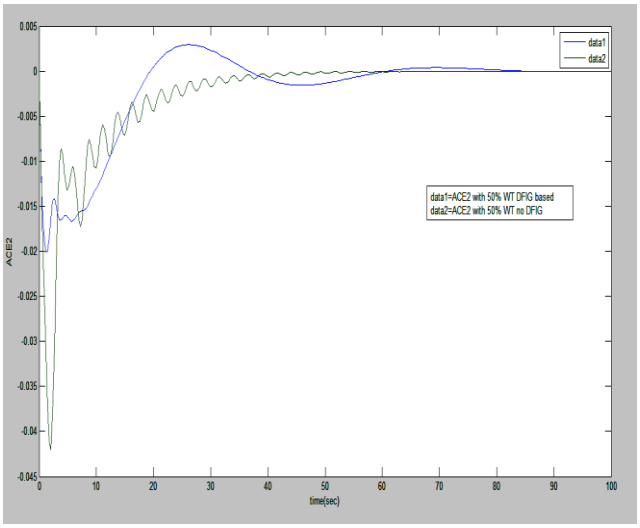

Fig. 17. Error in Area 1 with 2% sudden load change in favour of 50% wind penetration.

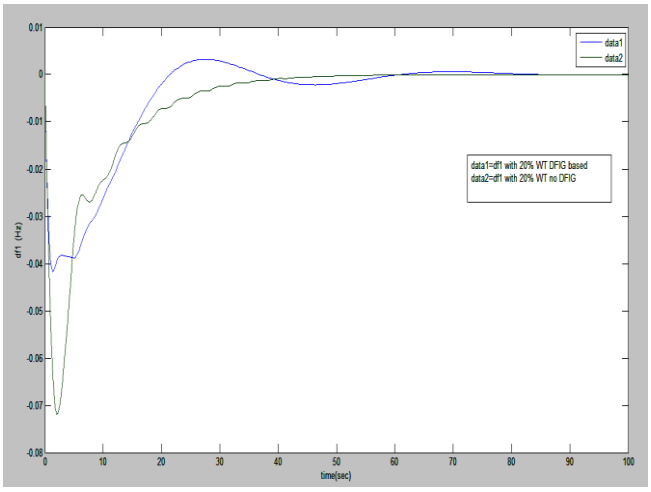

Fig. 18. Frequency regulations with and without DFIG for 20% wind penetration to area 1.

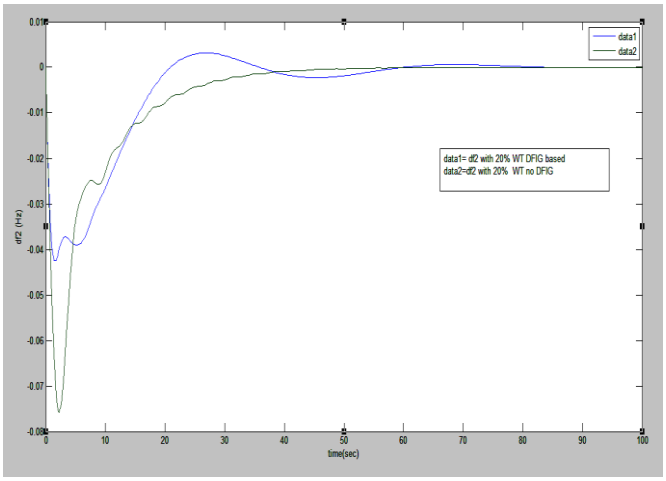

Fig. 19. Frequency regulation with and without DFIG for 20% wind penetration to area 2.

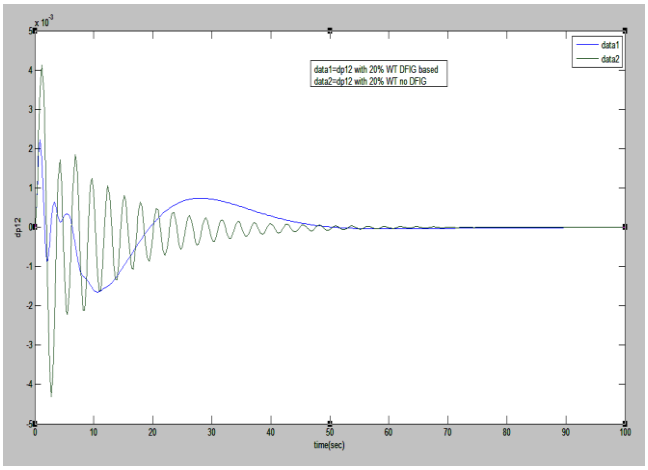

Fig. 20: Tie line incremental power for frequency regulation with20% wind penetration of area 2.

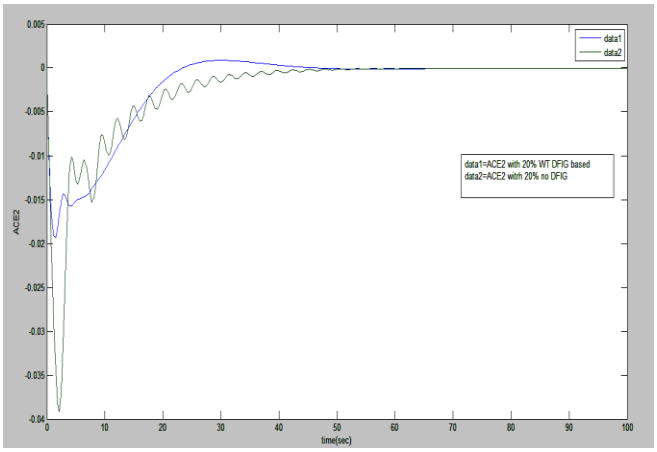

Fig. 21: Sudden load change in area2 for 20% wind penetration along with 2% Area errors.

6. CONCLUSION

The work is based on the dynamic Simulink model of two-area controller with and without DFIG-based WT. The work is carried out in favor of frequency response studies for 2% load perturbation in area 1 as well as area2. Whereas the Matlab frequency regulation model with optimum DFIG control parameters to two region systems is carried out for wind penetration between 20% and 50%. The frequency response is increased. It is detected. It is also found that when the degree of wind penetration levels up from 20% to 50%, higher penetration increases lower frequency peak output. The frequency response drops has been occurred by means of improved settling time with higher steady-state frequency error. Whereas AGC response along with DFIG is reduce the tie-line power incremental change. The frequency peak excursion is enhanced for 20% and 50% wind power DFIG based WT penetration. On the other hand after discharge of DFIG kinetic energy, its mechanical speed is cut down, and then DFIG output power is reduced. Therefore, the reduction in power production would be an additional pressure on AGC for greater DFIG penetration. It is found that with high wind energy dispersion, ACE is dropped. It is however difficult to include DFIG-based WTs in frequency regulation along with AGC in multi-area systems. DFIG-based WT opposes the fixed-speed wind turbine generator in this article, which contributes and improves frequency efficiency along with conventional support.

ACKNOWLEDGMENT

The authors are deeply appreciating the resources for their efforts from the Polytechnical Government Department of Electrical Engineering, U.P. (233001), India and Indian Technology Institute (Banaras Hindu University), Varanasi, Uttar Pradesh, India. This work is dedicated to the baby doll "Ananya Singh" and also lovely memories of the Grand Mother of first author "Patiraji Devi" who has no more from 24 November 2014 with us.

REFERENCES

[1] European Wind Energy Association, "Ocean of Opportunity".
[2] Reference from "EWEA wind is power", European Market for Wind Turbines Grows 23% in 2006.
[3] Darrell M. Dodge, *Illustrated history of wind power generation*, Littleton, Colorado.
[4] Reference from encyclopedia of alternative energy www.daviddarling.info.
[5] M. Aktarujjaman, M. E. Haque and M. Negnevitsky, "Contribution of DFIG-based wind farm to system frequency control," 2012 *7th International Conference on Electrical and Computer Engineering*, Dhaka, 2012, pp. 599-602.
[6] Jorge Morel, Hassan Bevrani, Teruhiko Ishii, and Takashi Hiyama, "A Robust Control Approach for Primary Frequency Regulation through Variable Speed Wind Turbines," IEEJ Transactions on Power and Energy, vol. 130, no. 11, pp. 1002-1009, 2010.
[7] University of Massachusetts at Amherst, *Introduction to the modeling of wind turbine, Wind Power system 2005*, John Wiley and Sons Ltd ISBN 0-470-85508-8 (HB).
[8] Siegfried Heier Kassel, *Wind energy Converter System*, John Wiley and Sons Ltd.
[9] Janaka Ekanayake and Nick Jenkins, "Comparison of the Response of Doubly Fed and Fixed-Speed Induction Generator Wind Turbines to Changes in Network Frequency," IEEE Transaction on Energy Conversion, vol. 19, no. 4, December 2004.
[10] R. Pena J.C.Clare, "Doubly Fed induction generator using back-to-back PWM converters and its application to variable speed wind-energy generation," Power Appl., vol. 143, No3, May 1996.
[11] J. G. Slootweg, S. W. H. de Haan, H. Polinder, and W. L. Kling, "General model for representing variable speed wind turbines in power system dynamics simulations," IEEE Transaction on Power Systems, Vol. 18, NO. 1, February 2003.
[12] Gillian Lalor, Julia Ritchie, Shane Rourke, Damian Flynn and Mark J. O, "Malley Dynamic Frequency Control with Increasing Wind Generation", Conference: Power Engineering Society General Meeting, IEEE, 2004.
[13] Rogério G. de Almeida and J. A. Peças Lopes, "Participation of Doubly Fed Induction Wind Generators in System Frequency Regulation", IEEE Transactions on Power Systems, vol. 22, No. 3, August 2007.
[14] Alan Mullane, and Mark O Malley, "The inertial response of induction-machine-based wind turbines", IEEE Transaction on Power Systems, VOL. 20, NO. 3, August 2005.
[15] Johan Morren, Sjoerd W. H. de Haan, Wil L. Kling, and J. A., "Wind Turbines Emulating Inertia and Supporting Primary Frequency Control", IEEE Transaction on Power Systems, vol. 21, no. 1, February 2006.
[16] Juan Manuel Mauricio, Alejandro Marano, Antonio Gómez-Expósito, and José Luis Martinez Ramos, "Frequency regulation contribution through variable-speed wind energy conversion systems," IEEE Transaction on Power Systems, Vol. 24, No. 1, February 2009.
[17] Andreoiu and K. Bhattacharya, "Robust tuning of power system stabilizers using Layapunove method based generic

algorithm," IEEE Proc. Gener Transaction Vol 149, No.5 Sep 2002.
[18] O. P. Bharti, R.K. Saket, S. K. Nagar, "Reliability Analysis of DFIG Based Wind Energy Conversion System," ICCAE'17, Proceedings of the 9th International Conference on Computer and Automation Engineering, pp: 313-317, Sydney, Australia, February 18 - 21, 2017.
[19] Om Prakash Bharti, R. K. Saket, S.K., "Controller Design of DFIG Based Wind Turbine by Using Evolutionary Soft Computational Techniques", Engineering, Technology & Applied Science Research, Vol. 7, No. 3, 2017, 1732-1736.
[20] Om Prakash Bharti, R. K. Saket, S.K. Nagar, "Controller Design for Doubly Fed Induction Generator Using Particle Swarm Optimization Technique," Renewable Energy, Science Direct, Elsevier 114 (Part B), 2017, 1394-1406, 2017.
[21] O. P. Bharti, R. K. Saket, S. K., "Controller Design for DFIG Driven by Variable Speed Wind Turbine Using Static Output Feedback Technique," Engineering, Technology & Applied Science Research, Vol. 6, No. 4, pp-1056-1061, 2016.
[22] D. P. Kothari and I. J. Nagrath, "Power system engineering" book, edition second, ISBN-13:978-0-07-0647916, 2008.
[23] Bevrani H, Habibi F, Babahajyani P, Watanabe M, Mitani Y., "Intelligent frequency control in an ac micro grid: online PSO-based fuzzy tuning approach", IEEE Trans Smart Grid 2012;3(4):1935–44.
[24] Kundur P., *Power system stability and control*, New York: McGraw Hill; 1994.
[25] Jalali M, Bhattacharya K., "Frequency regulation and AGC in isolated systems with DFIG-based wind turbines", In: Proc IEEE conf power and energy society general meeting, Canada; 2013.
[26] Jalali M., "DFIG based wind turbine contribution to system frequency control", Master thesis: Cabada University of Waterloo; 2011.
[27] Khani, Khosro and Shahgholian, Ghazanfar, "Analysis and optimization of frequency control in isolated micro grid with double-fed induction-generators based wind turbine", Journal of International Council on Electrical Engineering, Taylor & Francis, vol. 9(1), pp: 24-37, 2019.
[28] Teng, Weijun and Meng, Yongqing, "An improved control strategy to the frequency regulation of DFIG based wind turbine" Journal of Renewable and Sustainable Energy, vol.9, pp: 063-303, 2017.
[29] Aziz, Asma and Shafiullah, GM and Stojcevski, Alex and Mto, Amanullah, "Participation of DFIG based wind energy system in load frequency control of interconnected multi generation power system", book: Australasian Universities Power Engineering Conference (AUPEC), IEEE, 2014, pp: 1-6, 2014.
[30] Bhatt, Praghnesh and Long, Chao and Wu, Jianzhong and Mehta, Bhinal, "Dynamic participation of DFIG for frequency regulation in electrical power systems", Energy Procedia, Elsevier, vol.142, pp: 2183-2188, 2017.
[31] Gupta, Aditi, Yajvender Pal Verma, and Amit Chauhan. "Contribution of frequency linked pricing control on ALFC and AVR power system integrated with DFIG based wind farms," *Engineering Science and Technology, an International Journal*, vol. 23, no. 2 (2020): 325-333.
[32] Aktarujjaman, Md, M. E. Haque, S. Saha, and M. Negnevitsky, "Impact of DFIG Based Wind Generation on Grid Voltage and Frequency Support," In *2020 International Symposium on Power Electronics, Electrical Drives, Automation and Motion (SPEEDAM)*, pp. 42-46. IEEE, 2020.
[33] Singhal, Ashish Kumar, "Modelling of DFIG-based Wind Energy Conversion System," *Journal of Alternate Energy Sources and Technologies* 10, no. 3 (2020): 59-64.
[34] Yingyu, An, Yonggang Li, Jian Zhang, Ting Wang, and Changfeng Liu, "Enhanced Frequency Regulation Strategy for Wind Turbines Based on Over-speed De-loading Control" In *2020 5th Asia Conference on Power and Electrical Engineering (ACPEE)*, pp. 442-446. IEEE, 2020.

NOMENCLATURE

J	: Objective function
H	: Inertia constant of power system
He	: Inertia constant of wind generation
K_{AGC}	: AGC acceleration control gain
K_{df}	: AGC derivative controller gain
K_I	: Integral control gain of AGC
K_P	: Power gain
K_{pf}	: Gain of Proportional controller
K_{wi}	: DFIG integral gain
K_{wp}	: DFIG gain of proportional speed controller
P	: Perturbation vector
P_{mech}	: Mechanical output of wind turbine
Pu	: Per unit
P_{wind}	: Wind power
R	: Regulation drops
R_r	: Rotor radius
S	: Laplace variable
ΔP_D	: Increased demand of active power
ΔP_g	: Increased value of conventional power
ΔP_{12}	: Increased power shifted from adjacent region (area 1 to area 2).

APPENDIX

System Parameters Single Area:

He = $3P_U$.MW.sec, K_{agc} = 0.1, K_p = 62HZ/P_U, Kwi = 0.1, Kwp = 1.58, R = 3Hz/P_U.MW, Ta = 0.2Sec, T_h = 0.1Sec, T_p = 10se, T_r = 0.1Sec, T_t = 1Sec, Tw = 6Sec.

System Parameters Two Area:

He_1 = 3.5, He = 3.5, $Kagc_1$ = $Kagc_2$ = 0.05, Kp_1 = 62, wi_1 = 0.1, Kwp_1 = 1.58, Kp_2 = 62, Kwi_2 = 0.1, wp_2 = 1.61, R_1 = R_2 = 3, T° = 0.07, Ta_1 = Ta_2 = 0.2, Th_1 = Th_2 = 0.1, Tp_1 = 10, Tp_2 = 15, Tr_1 = Tr_2 = 0.1, Tt_1 = Tt_2 = 1, Tw_1 = Tw_2 = 6.